Over-expression of arginine vasopressin in magnocellular neurosecretory cells of hypothalamus and its potential relationship with development of diabetic nephropathy

Xianhua Li[1], Zhaoli Gao[2], Ling Xu[2], Baoying Li[2], Haiqing Gao[2]

[1]Department of Nephrology, Qi Lu Hospital of Shandong University, Jinan, China
[2]Department of Geriatrics, Qi Lu Hospital of Shandong University, Jinan, China

Submitted: 16 October 2017
Accepted: 27 January 2018

Arch Med Sci 2020; 16 (5): 1130–1139
DOI: https://doi.org/10.5114/aoms.2020.92402

Corresponding author:
Prof. Xianhua Li
Department of Nephrology
Qi Lu Hospital of Shandong University
107 Wenhua Xi Road
Jinan 250012, China
Phone: +86-0531-82169315
Fax: +86-0531-86927544
E-mail: lixianhua_sd@sohu.com

Abstract

Introduction: We aimed to assess our hypothesis that the expression changes of arginine vasopressin (AVP) in the magnocellular neurosecretory cells (MNCs) of hypothalamus and V2 receptor for AVP (RVP) in kidney may contribute to the pathogenesis of diabetic nephropathy (DN).

Material and methods: Twenty-five male Wistar rats were randomly assigned to the control group and the diabetes mellitus (DM) group. Periodic acid-Schiff (PAS) staining and electron microscopy were used for morphological studies. Immunohistochemical staining for glial fibrillary acidic protein (GFAP) is standard for visualization of reactive astrocytes in the hypothalamus. Hypothalamus was used for immunofluorescence of AVP. Kidney was used for immunohistochemical staining of RVP. Quantitative real-time reverse transcriptase polymerase chain reaction (qRT-PCR) was used for quantitative determinations of AVP mRNA in hypothalamus and RVP mRNA in kidney. Western blot was used to measure the protein expression of AVP in hypothalamus and RVP in kidney.

Results: Morphological studies showed abnormalities in kidney and hypothalamus in the DM group. The number of neurons and the gray value of astrocytes in hypothalamus in the DM group were markedly decreased. The expression level of AVP in hypothalamus and the expression level of RVP in kidney of DM rats were significantly increased. The positive correlations between the proteinuria and expression (mRNA and protein) of AVP, proteinuria and expression (mRNA and protein) of RVP, and the expression of AVP and RVP levels were found.

Conclusions: AVP was upregulated in the MNCs of hypothalamus and RVP was upregulated in kidney in streptozotocin-induced DM rats, indicating their potential roles in the development of DN.

Key words: diabetic nephropathy, arginine vasopressin, receptor for arginine vasopressin.

Introduction

Currently, diabetes mellitus (DM) is one of the biggest epidemics affecting human health. The alarming increase in the incidences of type 2 DM was reported to be attributed largely to vast changes in lifestyle, human behavior and increased lifespan [1]. The complications associated

with diabetes are a major cause of morbidity and mortality. Particularly, diabetic nephropathy (DN) is one of the major chronic microvascular complications in both type 1 and 2 DM patients, occurring in 20–40% of diabetic patients, and is also a leading cause of end-stage renal disease worldwide [2, 3].

The shunting of excess glucose is known to contribute to the generation of hyperglycemic end-organ damage. Klein *et al*. stated that two distinct mechanisms are involved in the pathogenesis of end organ damage in diabetes: one is the neurologically "passive" shunting of excess glucose that leads to oxidative damage and diffuse vascular injury; another is the "active" modulation of neuronal gene transcription in response to hyperglycemia, which changes neuronal structure and function, and in turn results in physiological deficits [4]. It indicates that the diabetic state can induce alterations in gene transcription within the central nervous system, including hypothalamic mononuclear cell (MNCs) and hippocampal neurons, which are strongly associated with the hyperglycemic end-organ damage.

Among them, an upregulated arginine vasopressin (AVP) level was found in the diabetic supraoptic nucleus and was reported to play a vital role in neuronal function and can drive diabetes-related pathogenesis and end-organ damage [4]. Arginine vasopressin, a small nine-amino-acid peptide that is synthesized in specific neurons in the paraventricular and supraoptic nuclei, is stored in the neurohypophysis. It responds to comparatively large reductions in blood volume or to minor increases in plasma osmolality [5]. A previous study suggested that block of abnormal sodium channel or normalization of sodium channel expression activity in MNCs of the hypothalamus could decrease AVP secretion, and might thereby attenuate the hyperfiltration, renal hypertrophy and albuminuria, finally slowing the onset of DN [4]. Arginine vasopressin exerts its actions via vasopressin receptors. Type V2 and type V1a are two main types of AVP receptors found in the kidney, and particularly, the major effect of AVP on the kidney is to favor water reabsorption in the collecting duct through binding to V2 receptor for AVP (RVP) [6, 7]. Therefore, according to the findings mentioned above, we speculated that the expression changes of AVP in the MNCs of hypothalamus and RVP in kidney may contribute to DN pathogenesis.

To test the hypothesis, streptozotocin (STZ) was used to induce diabetic rats, and the main characteristics of DM and the changes in the DN markers were detected to validate the successful construct of the DN model. Periodic acid-Schiff (PAS) staining and electron microscopy were used for the morphological studies of kidney and hypothalamus. Immunohistochemical staining for glial fibrillary acidic protein (GFAP) is standard for visualization of reactive astrocytes in the hypothalamus.

Material and methods

Animals

Thirty male Wistar rats (180–220 g) were obtained from the Animal Centre of Shandong University. Rats were kept in individual cages on a 12 h-light/12 h-dark cycle with the temperature in the range of 20°C to 22°C and supplied with free food and water. This study was approved by the Animal Care Committee of Shandong University.

Induction of diabetic rats

Twenty rats received a single tail vein injection of STZ (55 mg/kg), which was freshly dissolved in sodium citrate buffer (0.1 M, pH 4.5) after fasting for 12 h overnight. Ten rats in the control group received a single tail vein injection of 0.1 M citrate buffer alone. The blood samples were collected from the tail of each rat daily. By using a glucose oxidase-impregnated test strip and a reflectance meter (One Touch II, Lifescan, Inc., Milpitas, California, USA), glucose concentration was measured. Diabetic rats were chosen based on the blood glucose level (≥ 16.7 mM after 5 days). In our study, 2 rats (< 16.7 mM) were excluded from the investigation.

Tissue collection

After 24 weeks, the rats were anesthetized and intraperitoneally perfused as described in the previous study [8]. After 30 min of perfusion, hypothalami were removed and frozen immediately. The kidneys were perfused with ice-cold PBS via the abdominal aorta as described previously [9].

The brain was thawed sufficiently to block into the forebrain and brainstem using a razor blade, and the hypothalamus was picked out for sectioning preparation. Tissue blocks were embedded in Tissue-Tek (Miles Scientific, Naperville, IL, USA) immediately and placed on a quick-freeze platform at –40°C. Half of all hypothalamus tissues were put in 2% formaldehyde and embedded in paraffin; afterwards, 4 µm sections were serially cut and stained for immunohistochemical and morphological studies. Another half of hypothalamus tissues were used for Western blot and quantitative real-time reverse transcriptase polymerase chain reaction (qRT-PCR) analysis.

Assessments of renal function-associated indexes

After 24 weeks, the rats underwent the analysis of renal function. The serum fasting plasma

glucose (FPG) level, serum creatinine and urinary creatinine were detected by an automatic biochemical analysis instrument (DVI 1650; Bayer, Leverkusen, Germany). The level of glycosylated hemoglobin A_{1c} (HbA_{1c}) was measured using the high performance liquid chromatography method (HA-8160 HbA_{1c} Analyzer; Menarini Diagnostics, Florence, Italy). To measure advanced glycation end products (AGEs) in serum, a fluorescence spectrophotometer (Hitachi F-2500; Hitachi, Tokyo, Japan) was used to determine specific fluorescence by measuring 440 nm emissions after excitation at 370 nm [10]. To collect urine samples, the rats had free access to tap water but were deprived of food for 24 h in individual cages before being killed. The urine samples were centrifuged (1500 × *g*, 15 min) and supernatants were stored in polyethylene containers at –20°C. Urinary albumin concentrations in fresh urine samples were determined by enzyme-linked immunosorbent assay (ELISA, Nephrat II; Exocell, Philadelphia, PA), and this value was multiplied by urine volume to get the total 24-h urine albumin excretion (mg).

PAS staining and electron microscope studies

By using PAS staining and electron microscopy, the renal pathological changes were examined. The kidneys were immersion-fixed and embedded in paraffin, and 4 µm sections were stained with PAS reagent. For electron microscope examination, the renal cortex was cut into pieces and prefixed for 4 h, postfixed for 1 h and embedded in Epon 812. Ultra-thin sections were examined using an H-800 electron microscope (Hitachi). Messenia matrix expansion was determined as PAS-positive materials presented in the mesangial region excluding cellular elements. By using Leica QWin V3 image analysis software, the percentage of PAS-positive area in each glomerulus was analyzed.

Western blot

Protein was collected from hypothalamus and renal tissues that were lysed in radioimmunoprecipitation buffer (RIPA) containing protease inhibitors at 4°C for 30 min. Cell lysates were prepared with a RIPA lysis buffer kit (Santa Cruz Biotechnology, Inc., Dallas, TX, USA), and the protein concentrations were quantified using a Bio-Rad protein assay (Bio-Rad Laboratories, Inc., Hercules, CA, USA). Proteins (30 µg) were separated on 8% SDS-PAGE and transferred to polyvinylidene difluoride membranes (Amersham; GE Healthcare, Chicago, IL, USA). The membranes were blocked in 5% non-fat milk (Merck KGaA, Darmstadt, Germany) overnight at 4°C. Transferred membranes were then stained with the following primary: anti-AVP (1 : 400, R&D Systems, Minneapolis, MN, USA), anti-RVP (1 : 200, Biolegend, San Diego, CA, USA) and anti-β-actin (1 : 500, Abcam, Cambridge, UK). Subsequently, protein bands were detected by incubation with a horseradish peroxidase-conjugated secondary antibody (1 : 1,000; Beijing Zhongshan Golden Bridge Biotechnology Co., Ltd., Beijing, China) at room temperature for 1 h. Signals were detected using an enhanced chemiluminescence kit (Wuhan Boster Biotechnology Co., Ltd, Wuhan, China) and exposed to Kodak X-OMAT film (Kodak, Rochester, NY, USA). Each experiment was performed at least three times and the results were analyzed using Alpha View Analysis Tools (AlphaView SA software, ProteinSimple, Santa Clara, CA). β-actin served as the loading control.

Immunohistochemistry and immunofluorescence

Immunohistochemistry was performed as previously described [8]. Briefly, sections were deparaffinized, dehydrated, and the endogenous peroxidase was blocked by incubation with hydrogen peroxide. After being washed, the sections were incubated in sheep serum for 5 min, followed by incubation with rabbit anti-antibodies anti-RVP (1 : 200, Biolegend) and anti-GFAP (1 : 400, Wuhan Boster Biotechnology Co.) overnight, respectively. Sections were then incubated with biotinylated anti-rabbit IgG (1 : 1,000, Origene Technologies, Inc, Beijing, China). Two observers blinded to the brain conditions were enrolled to analyze the immunohistochemical-stained brain slides. For AVP expression in the hypothalamus, immunofluorescence was performed as previously described, with some alterations [11]. Slices were washed in PBS for 30 min at room temperature and blocked with 10% normal goat serum before being incubated in a rabbit monoclonal antibody against AVP (1 : 100; Phoenix Pharmaceuticals, Burlingame, CA, USA) diluted in 0.01 mol/l PBS containing 1% bovine serum albumin, 0.02% sodium azide, and 0.03% Triton X-100 at 4°C overnight. After rinsing, the sections were incubated in secondary antibody solutions (1 : 200, Cy3-conjugated goat anti-rabbit IgG; Sigma, St. Louis, MO, USA) for 1 h at room temperature. Nuclei were stained with Hoechst-33258 dye (MedChem Express, Monmouth Junction, NJ, USA). Then the sections were examined by a fluorescence microscope (Nikon E-1000; Nikon, Tokyo, Japan).

qRT-PCR

Total RNA was extracted from hypothalamus tissues and renal tissues using Trizol reagent (Life Technologies Inc., Rockville, MD, USA) and pro-

cessed for cDNA synthesis using the TaqMan Reverse Transcription Reagents kit (Applied Biosystems, Shanghai, China). The PCR primers and TaqMan probes were designed according to the published sequence data from the NCBI database or by using software. Primers sequences of AVP: forward: 5'-CACCTCTCGCCTGCTACTTCC-3', and reverse: 5'-GGGCAGGTAGTTCTCCTCCT-3' (Product 199 bp). Primer sequences of RVP: forward: 5'-CGTGGCTAGGTAGGTAGGGATGAA-3', and reverse: 5'-AGCTGAGGCAGTACCTGGAA-3' (Product 202 bp). The reactions were performed in an ABI PRISM 7900HT Sequence Detection System with the following amplification procedure: pre-denaturation at 95°C for 3 min; denaturation at 95°C for 30 s, annealing at 60°C for 40 s and extension at 72°C for 30 s for AVP and 1 min for RVP, with 35 cycles; and final extension at 72°C for 7 min. Data were normalized to GAPDH and compared to control rats (defined as 1.0-fold).

Statistical analysis

Data were expressed as mean ± standard deviation (SD). Student's *t* test was performed to compare the significant differences between the control and the diabetic groups. The correlation between AVP and RVP at both protein and gene expression levels was analyzed by Pearson correlation tests. Statistical analyses were performed using the SPSS statistical software package standard version 16.0 (SPSS, Inc., Chicago, IL, USA). $P < 0.05$ was considered to indicate a statistically significant difference.

Results

Animal characteristics

In comparison with control animals, the diabetic rats had reduced body weight; significant differences were observed after 16 weeks (Figure 1). As shown in Table I, the serum FPG level, the percentage of HbA_{1c}, the levels of AGEs, endogenous creatinine clearance rate (Ccr) and 24-h urinary albumin excretion in the DM group were markedly higher than those in the control group. Importantly, we also found that the kidney/body weight ratio, which can partially reflect the degree of renal failure, was significantly higher in the DM group than that in the control group.

Morphological studies of diabetic kidney in rats

Glomerular injury (diffuse and nodular glomerulosclerosis) was a prominent feature of diabetic rats. In our study, the PAS-positive materials were increased in the kidneys of the DM group, indicating that accumulation of extracellular matrix was greater in the DM group than the control group (Figures 2 A, B). In addition, the percentage of PAS in the glomerulus and tubule of the DM group were significantly higher than that in the control group (Table II). By electron microscopy, the glomeruli morphological changes were assessed. Segmental thickness of glomerular basement membranes, widely fused podocytes, excessively deposited mesangial matrix and injured organoid were observed in the DM group. No significant abnormalities were observed in the control group (Figures 2 C, D).

Morphological studies of hypothalamus in rats

The layers of neurons were not intact, the nuclei of neurons were shrunk, and more pink-colored areas (the plasma of neurons) were detected in the DM group in the morphological study (Figures 3 A, B). The number of neurons in hypothal-

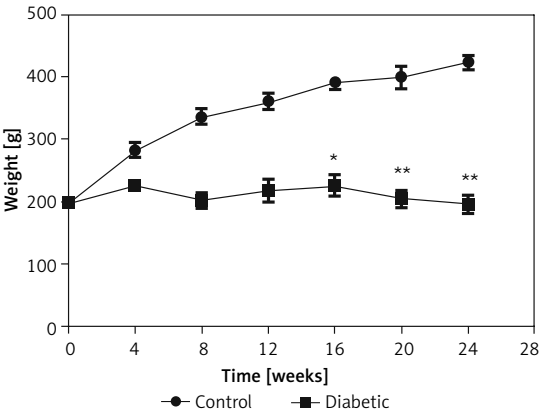

Figure 1. Rat body weight in diabetes mellitus (DM) and control groups at 0, 4, 8, 12, 16, 20 and 24 weeks. $N = 18$ in DM group and $n = 10$ in control group

Data are shown as mean ± SD, ˚p < 0.05 and ¨p < 0.01 compared to control group.

Table I. Renal dysfunction changes in rats

Group	*N*	FPG [mmol/l]	HbA_{1c} (%)	AGEs [AU/mg]	Ccr [ml/min]	24 h urinary albumin excretion [mg/day]	Kidney/body weight [× 10^{-3}]
Control	10	6.99 ±0.87	5.61 ±0.72	0.017 ±0.004	1.99 ±0.32	16.23 ±3.68	3.35 ±0.19
DM	8	23.03 ±0.94**	11.40 ±2.13**	0.074 ±0.006**	5.10 ±1.14**	44.95 ±14.57**	5.49 ±0.18**

*Data are shown as mean ± SD. **p < 0.01 vs. control group. DM – diabetes mellitus.*

Table II. Morphometric analysis of PAS staining (extracellular matrix)

Group	*N*	Extracellular matrix	
		Glomeruli (%)	Tubule (%)
Control	10	3.85 ±0.25	1.12 ±0.38
DM	8	8.71 ±0.45**	4.91 ±0.45**

Data are shown as mean ± SD. ¨p < 0.01 vs. control group. DM – diabetes mellitus.

amus in the DM group was markedly decreased as compared to the control group ($p < 0.05$) (Figure 3 C). Immunohistochemical studies were performed; the results showed that the gray value of astrocytes in hypothalamus in the DM group was significantly decreased as compared to the control group ($p < 0.01$) (Figure 3 D) and the number of GFAP positive cells in hypothalamus in the DM group was increased as compared to the control group ($p < 0.01$) (Figure 3 E).

Expression levels of AVP in hypothalamus and levels of RVP in kidney of rats

The qRT-PCR results showed that the expression of AVP mRNA in hypothalamus of DM rats was significantly increased as compared to the controls ($p < 0.01$) (Figure 4 A). The expression of RVP mRNA in kidney of DM rats was also significantly increased as compared to the control rats ($p < 0.01$) (Figure 4 B). The immunofluorescence analysis revealed that the expression of AVP in hypothalamus of DM rats was increased as compared to the controls ($p < 0.01$) (Figure 4 C). Similarly, the expression of RVP in kidney of DM rats was increased when compared to the normal controls ($p < 0.01$) (Figure 4 D). The Western blot anal-

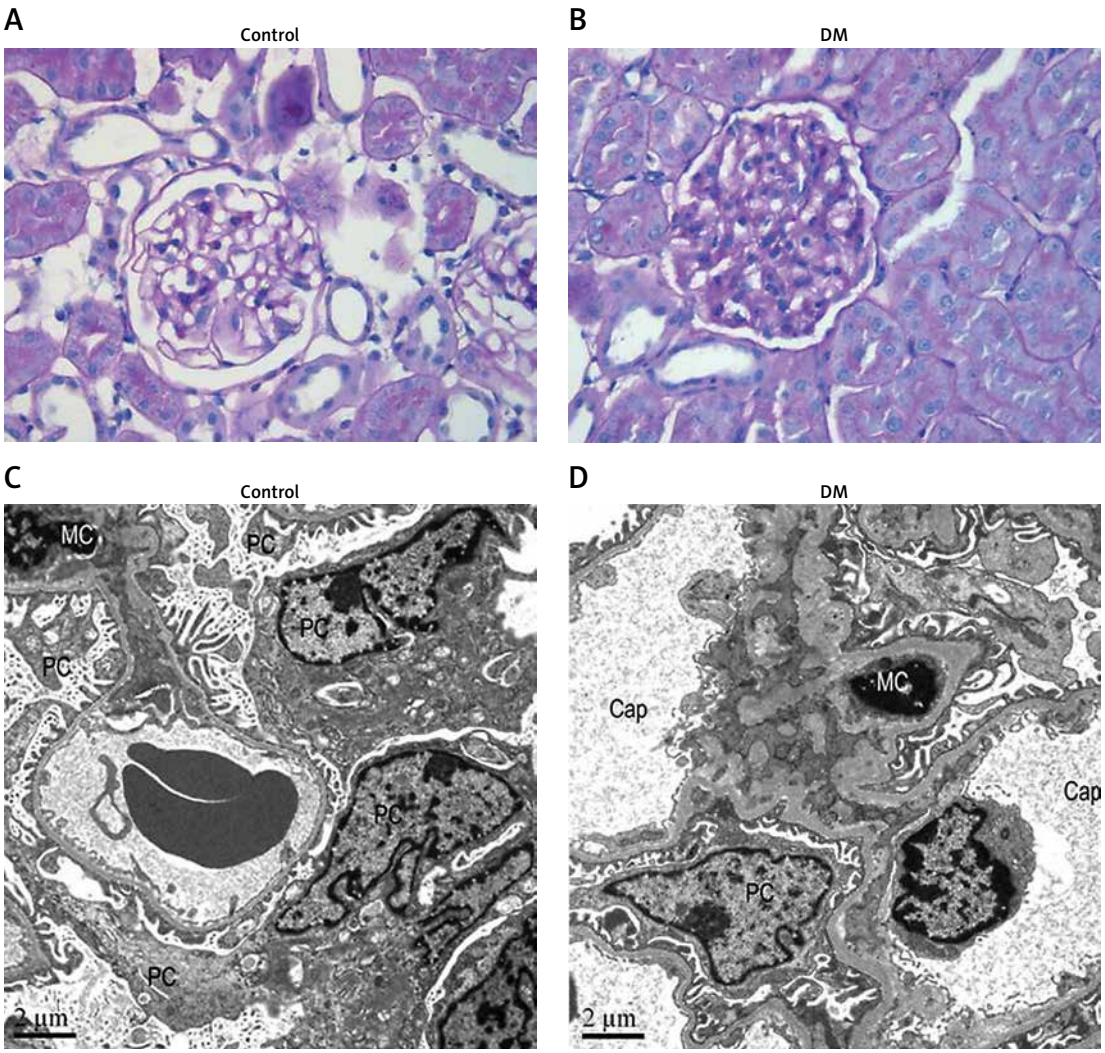

Figure 2. Morphological studies of diabetic kidney in rats. **A** – Light microscopic findings of renal morphological changes in control rats by periodic acid-Schiff staining (PAS 400×). **B** – Light microscopic findings of renal morphological changes in diabetes mellitus (DM) rats by PAS staining (400×). **C** – Electron microscopic findings of renal ultramicrostructure changes in control rats (12 000×, scale bar: 2 µm). **D** – Electron microscopic findings of renal ultramicrostructure changes in DM rats (12 000×, scale bar: 2 µm). *N* = 18 in DM group and *n* = 10 in control group

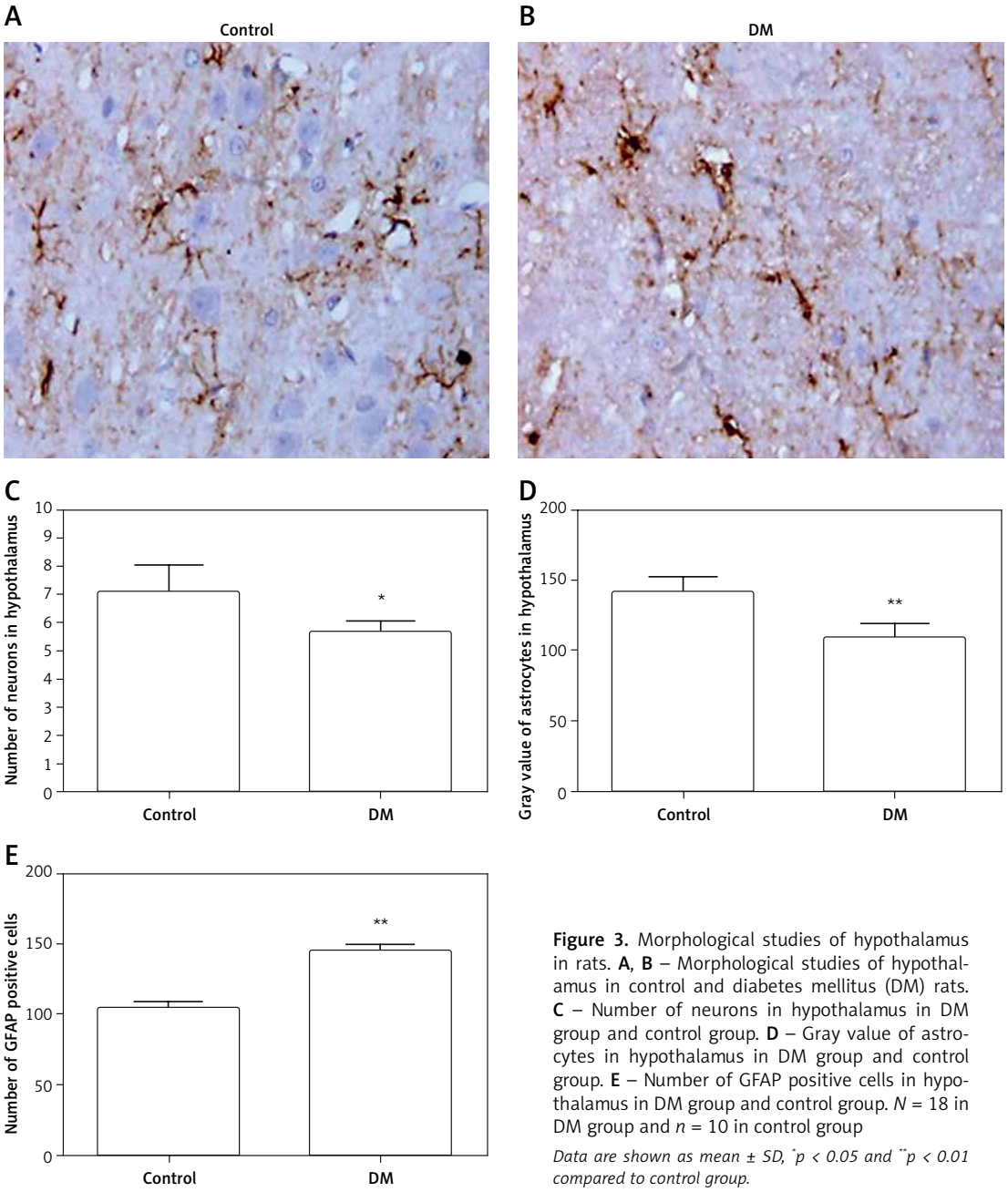

Figure 3. Morphological studies of hypothalamus in rats. **A**, **B** – Morphological studies of hypothalamus in control and diabetes mellitus (DM) rats. **C** – Number of neurons in hypothalamus in DM group and control group. **D** – Gray value of astrocytes in hypothalamus in DM group and control group. **E** – Number of GFAP positive cells in hypothalamus in DM group and control group. *N* = 18 in DM group and *n* = 10 in control group

*Data are shown as mean ± SD, *p < 0.05 and **p < 0.01 compared to control group.*

ysis showed that the protein expression levels of AVP and RVP in DM rats were markedly increased as compared to the control rats (Figures 4 E, F), which was in accordance with the immunofluorescence, immunochemistry and qRT-PCR results.

Correlation between AVP, RVP expression and proteinuria

Positive correlations between the proteinuria and mRNA/protein expression of AVP were found (Figures 5 A, B). The proteinuria was also positively correlated with the mRNA/protein expression of RVP (Figures 5 C, D). Also there were positive correlations between the mRNA/protein expression of AVP and RVP mRNA/protein levels (Figures 5 E, F).

Discussion

Streptozotocin is widely used to induce diabetes because STZ-induced experimental diabetic rats exhibit well-characterized diabetic complications and sustained hyperglycemia with a low incidence of mortality [12–14]. Here, STZ-induced diabetes rats were constructed to investigate the potential role of AVP and RVP in the development of DN. Diabetic nephropathy is characterized by excessive amassing of extracellular matrix, an increased amount of mesangial matrix, along with tubular

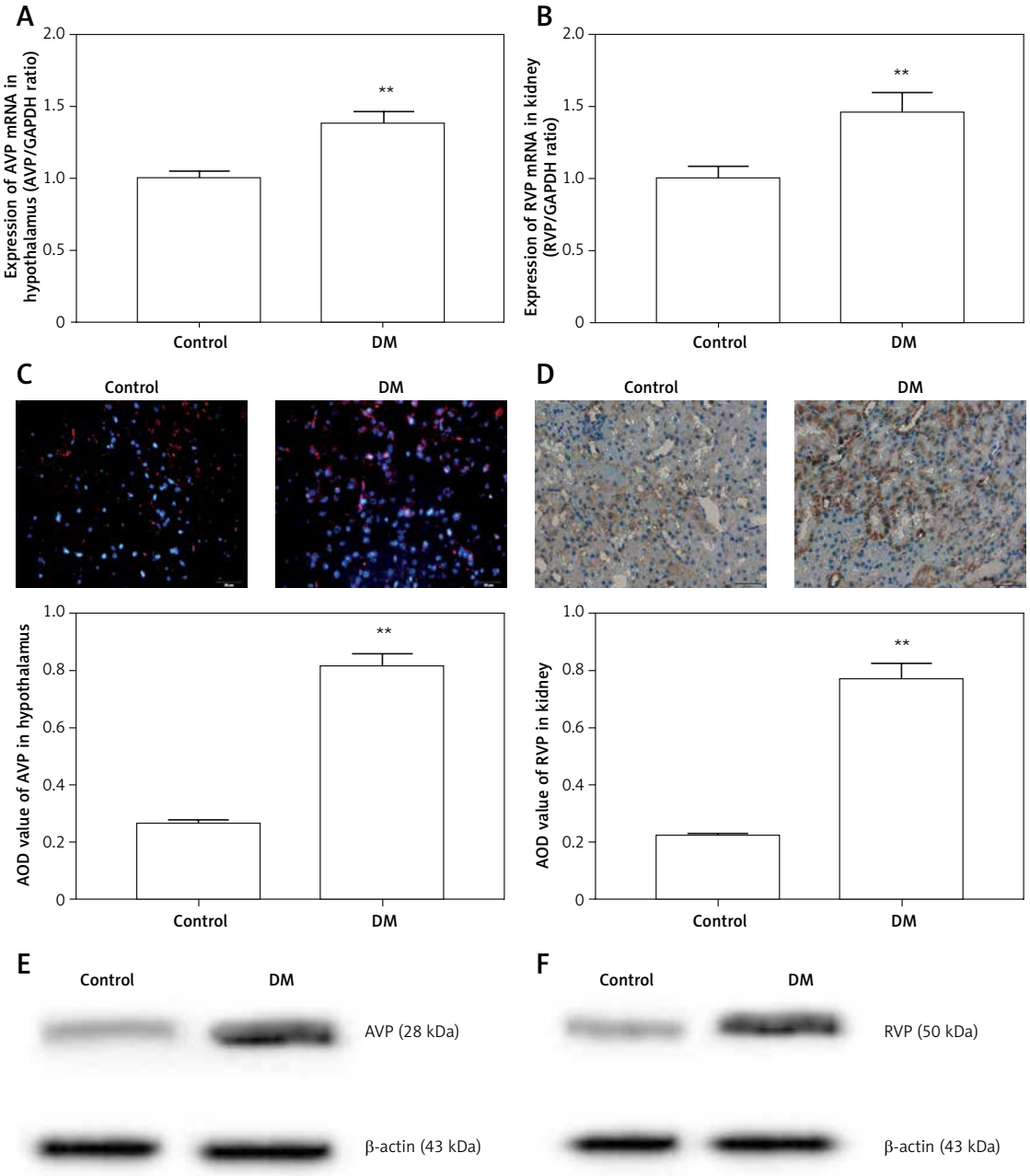

Figure 4. Expression levels of AVP in hypothalamus and levels of RVP in kidney of rats. **A** – The qRT-PCR analysis of expression of AVP mRNA in hypothalamus of diabetes mellitus (DM) rats and controls. **B** – The qRT-PCR analysis of expression of RVP mRNA in kidney of DM rats and control rats. GAPDH served as the loading control of qRT-PCR. **C** – Immunofluorescence analysis of AVP expression in hypothalamus of DM rats and controls. AVP was stained in red (Cy3-conjugated), and nuclei were stained with Hoechst-33258 dye (blue). Average optical density (AOD) value of AVP in hypothalamus of DM rats is shown below. Scale bar: 20 µm. **D** – Immunochemistry analysis of RVP expression in kidney of DM rats and normal controls. AOD value of RVP in kidney of DM rats is shown below. Scale bar: 20 µm. **E** – Western blot analysis of AVP protein expression level in DM rats and control rats. **F** – Western blot analysis of RVP protein expression level in DM rats and control rats. β-actin served as the loading control of Western blot. N = 18 in DM group and n = 10 in control group

Data are shown as mean ± SD, ¨$p < 0.01$ compared to control group.

basement membranes and thickening of the glomerular [15]. In this study, rats exhibited a decrease in body weight and an increase in FPG accompanied by polyuria and polydipsia (data not shown) following STZ injection, indicating the success of establishment of STZ-induced DM rats. In addition, these STZ-induced diabetic rats had a markedly higher percentage of HbA_{1c}, level of AGEs, Ccr, 24-h urinary albumin excretion and kidney/body weight ratio than those in the control group. Also, the accumulation of extracellular matrix in the kidneys of DM group was greater in the DM group than the

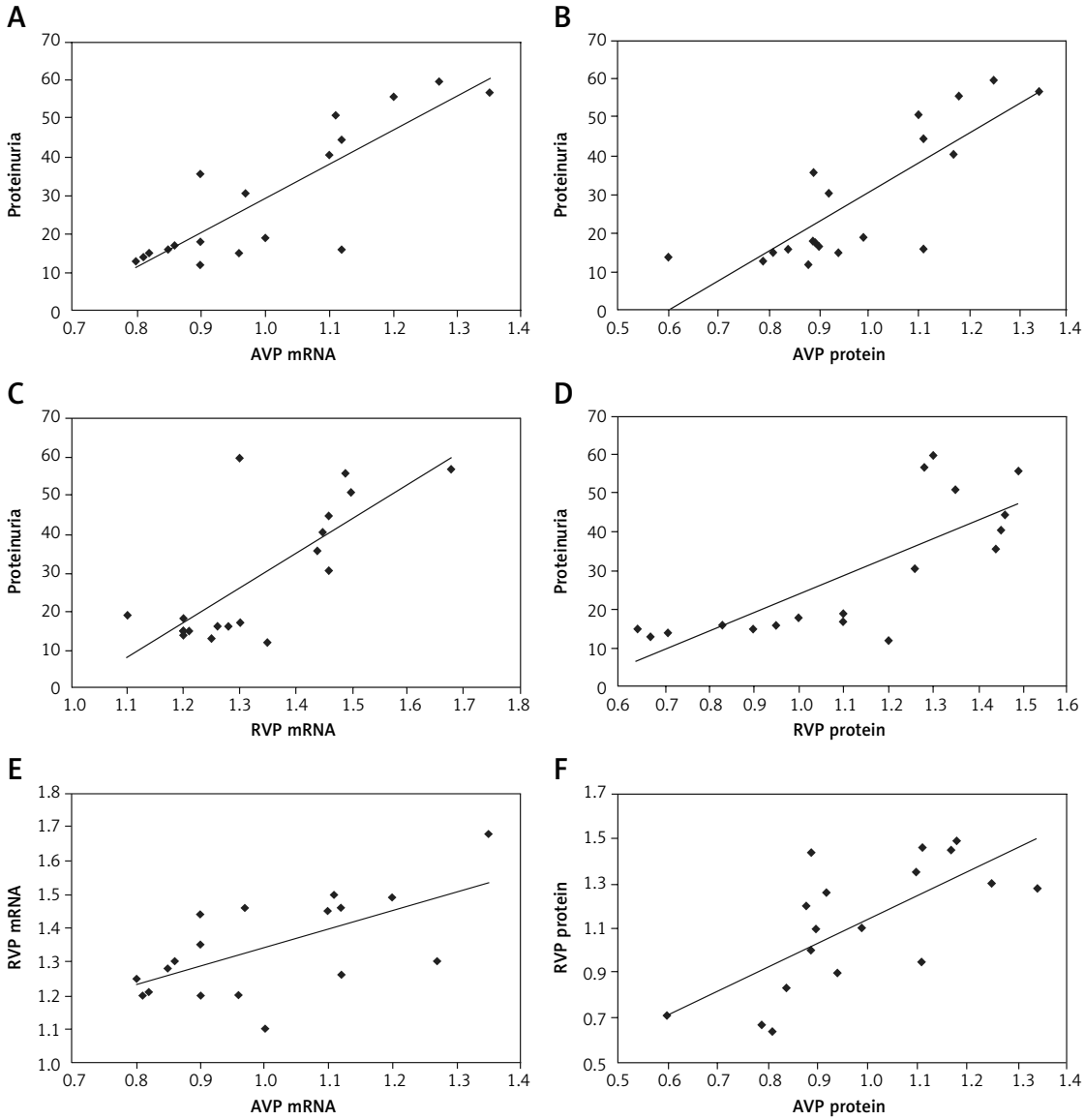

Figure 5. The correlation between AVP, RVP expression and proteinuria. **A** – The positive correlation between proteinuria and mRNA expression of AVP. **B** – The positive correlation between proteinuria and protein expression of AVP. **C** – The positive correlation between proteinuria and mRNA expression of RVP. **D** – The positive correlation between proteinuria and protein expression of RVP. **E** – The positive correlation between mRNA expression of AVP and RVP. **F** – The positive correlation between protein expression of AVP and RVP. *N* = 18 in DM group and *n* = 10 in control group

control group. The percentage of PAS in the glomerulus and tubule of the DM group was significantly higher than that in the control group. Segmental thickness of glomerular basement membranes, excessively deposited mesangial matrix, widely fused podocytes and injured organoid were observed in the DM group. Our findings demonstrated that STZ-induced DM rats exhibited the main characteristics of DM and the changes in the DN markers, indicating the success of establishment of DM-related DN rat models, which was partially consistent with the previous studies [16–19].

Arginine vasopressin is a peptide neuroendocrine hormone secreted from the hypothalamus and stored in the posterior pituitary before its release into the circulation. Any AVP present in peripheral circulation mainly originated from this source. Our morphological study showed that the DM rats displayed shrunk nuclei of neurons, incomplete layers of neurons, and a markedly decreased number of neurons as compared to the control group. A previous study indicated that although upregulation of AVP production in response to acute hyperosmolality is adaptive, prolonged overstimulation of AVP-producing neurons in chronic diabetes could lead to neurodegeneration and apoptosis [20]. It may suggest that the neurodegeneration and apoptosis are due to the upregulation of AVP.

Astrocytes are the most abundant cell type in the mature brain and have the ability to provide

trophic and metabolic support to neurons. Astrocytes play an important role in brain glucose metabolism, neuronal homeostasis and transmission, and also exert effects on the maintenance of the extracellular environment and brain-blood barrier, as well as in the regulation of cerebral microcirculation [21]. It is known that increased astrocyte reactivity can stimulate production of trophic factors, which in turn enhances neuronal survival, which represents an adaptation to hyperglycemia and changes in glucose homoeostasis [22]. Our results showed that the gray value of GFAP-positive astrocytes in hypothalamus in the DM group was markedly decreased as compared to the control group, indicating the link between enhanced expression of AVP and reduced amounts of astrocytes in hypothalamus.

Arginine vasopressin introduces water-permeable channels into the renal collecting duct, which acutely limits or prevents an increase in serum osmolality. Previous studies have shown that AVP plays a role in the accompanying progressive renal damage and induction of albuminuria due either to severe reduction in renal mass or to DN [23, 24]. Arginine vasopressin also contributes to the protein-induced glomerular hyperfiltration, a factor known to promote albumin leakage through the glomerular filter, and glomerulosclerosis [25–27]. Moreover, AVP-mediated increase of urinary albumin excretion in healthy rats and humans may be due to the increased glomerular leakage that requires functional RVP [23]. Receptors for AVP reside in renal collecting ducts and are responsible for water retention [28, 29]. Long-term overactivation of RVP by chronic high serum concentrations of AVP results in glomerular hyperfiltration, albuminuria, and renal hypertrophy. In contrast, these changes are not seen in AVP-deficient animals with STZ-induced diabetes. Additionally, normalization of AVP concentrations was reported to prevent the development of these changes [4, 30, 31]. Here, we found that the expression level of AVP in hypothalamus and the expression level of RVP in kidney of DM rats were significantly increased as compared with the control rats. Positive correlations between proteinuria and expression of AVP, proteinuria and expression of RVP, and expression of AVP and RVP were also found.

Interestingly, AVP is involved in neurohormonal activation, one of the major factors in this process of cardiorenal syndrome. Mechanically, AVP acts on RVPs located in the renal collecting ducts, causing fluid retention and deterioration of heart failure [32]. Furthermore, our results above suggested that the neurodegeneration and apoptosis may be due to the upregulation of AVP. In addition, a recent study reported that disruption of cardiac cholinergic neurons enhances susceptibility to ventricular arrhythmias [33]. Accordingly, we speculated that AVP may exert a destructive role in heart neurons. Further investigation of this hypothesis is required. Moreover, this study focused on AVP and RVP expression in STZ-induced DM rats; a human study regarding this subject needs to be further carried out.

In conclusion, the present study demonstrated that AVP expression was upregulated in the MNCs of hypothalamus in STZ-induced DM rats compared with the normal controls. Furthermore, RVP was also upregulated in kidney in DM rats induced by STZ. Our results indicated the potential roles of AVP and RVP in the development of DN, shedding new light on the molecular mechanism underlying DN.

Acknowledgments

This study was supported by a grant from the Natural Science Foundation of QiLu Hospital of Shandong University (No. 2015QLMS14).

We thank Prof. Junhui Zhen from Shandong University for technical assistance and insightful discussion.

Conflict of interest

The authors declare no conflict of interest.

References

1. Zheng Y, Ley SH, Hu FB. Global aetiology and epidemiology of type 2 diabetes mellitus and its complications. Nat Rev Endocrinol 2018; 14: 88-98.
2. Azushima K, Gurley S, Coffman T. Modelling diabetic nephropathy in mice. Nat Rev Nephrol 2018; 14: 48-56.
3. Conserva F, Gesualdo L, Papale M. A systems biology overview on human diabetic nephropathy: from genetic susceptibility to post-transcriptional and post-translational modifications. J Diabetes Res 2016; 2016: 7934504.
4. Klein JP, Waxman SG. The brain in diabetes: molecular changes in neurons and their implications for end-organ damage. Lancet Neurol 2003; 2: 548-54.
5. Rotondo F, Butz H, Syro LV, et al. Arginine vasopressin (AVP): a review of its historical perspectives, current research and multifunctional role in the hypothalamo-hypophysial system. Pituitary 2016; 19: 345-55.
6. Burrell LM, Risvanis J, Dean RG, Patel SK, Velkoska E, Johnston CI. Age-dependent regulation of renal vasopressin V(1A) and V(2) receptors in rats with genetic hypertension: implications for the treatment of hypertension. J Am Soc Hypertens 2013; 7: 3-13.
7. Kim YB, Kim WB, Jung WW, et al. Excitatory GABAergic action and increased vasopressin synthesis in hypothalamic magnocellular neurosecretory cells underlie the high plasma level of vasopressin in diabetic rat. Diabetes 2018; 67: 486-95.
8. Xu L, Li B, Cheng M, et al. Oral administration of grape seed proanthocyanidin extracts downregulate RAGE dependant nuclear factor-kappa BP65 expression in the hippocampus of streptozotocin induced diabetic rats. Exp Clin Endocrinol Diabetes 2008; 116: 215-24.
9. Li BY, Cheng M, Gao HQ, et al. Back-regulation of six oxidative stress proteins with grape seed proanthocyani-

din extracts in rat diabetic nephropathy. J Cell Biochem 2008; 104: 668-79.
10. Cai Q, Li B, Yu F, et al. Investigation of the protective effects of phlorizin on diabetic cardiomyopathy in db/db mice by quantitative proteomics. J Diabetes Res 2013; 2013: 263845.
11. Zhu J, Chen Z, Zhu L, Meng Z, Wu G, Tian Z. Arginine vasopressin and arginine vasopressin receptor 1b involved in electroacupuncture-attenuated hypothalamic-pituitary-adrenal axis hyperactivity in hepatectomy rats. Neuromodulation 2016; 19: 498-506.
12. Barman S, Pradeep SR, Srinivasan K. Zinc supplementation alleviates the progression of diabetic nephropathy by inhibiting the overexpression of oxidative-stress-mediated molecular markers in streptozotocin-induced experimental rats. J Nutr Biochem 2017; 54: 113-29.
13. Barrière DA, Noll C, Roussy G, et al. Combination of high-fat/high-fructose diet and low-dose streptozotocin to model long-term type-2 diabetes complications. Sci Rep 2018; 8: 424.
14. Bhadri N, Razdan R, Goswami SK. Nebivolol, a beta-blocker abrogates streptozotocin-induced behavioral, biochemical, and neurophysiological deficit by attenuating oxidative-nitrosative stress: a possible target for the prevention of diabetic neuropathy. Naunyn Schmiedebergs Arch Pharmacol 2018; 391: 207-17.
15. Kanwar YS, Wada J, Sun L, et al. Diabetic nephropathy: mechanisms of renal disease progression. Exp Biol Med (Maywood) 2008; 233: 4-11.
16. Kelly DJ, Zhang Y, Moe G, Naik G, Gilbert RE. Aliskiren, a novel renin inhibitor, is renoprotective in a model of advanced diabetic nephropathy in rats. Diabetologia 2007; 50: 2398-404.
17. Nakagawa T, Sato W, Glushakova O, et al. Diabetic endothelial nitric oxide synthase knockout mice develop advanced diabetic nephropathy. J Am Soc Nephrol 2007; 18: 539-50.
18. Ota T, Takamura T, Ando H, Nohara E, Yamashita H, Kobayashi K. Preventive effect of cerivastatin on diabetic nephropathy through suppression of glomerular macrophage recruitment in a rat model. Diabetologia 2003; 46: 843-51.
19. Si X, Li P, Zhang Y, Zhang Y, Lv W, Qi D. Renoprotective effects of olmesartan medoxomil on diabetic nephropathy in streptozotocin-induced diabetes in rats. Biomed Rep 2014; 2: 24-8.
20. Klein JP, Hains BC, Craner MJ, Black JA, Waxman SG. Apoptosis of vasopressinergic hypothalamic neurons in chronic diabetes mellitus. Neurobiol Dis 2004; 15: 221-8.
21. Lechuga-Sancho AM, Arroba AI, Frago LM, et al. Reduction in the number of astrocytes and their projections is associated with increased synaptic protein density in the hypothalamus of poorly controlled diabetic rats. Endocrinology 2006; 147: 5314-24.
22. Baydas G, Nedzvetskii VM, Yasar A, Kirichenko SV. Increase of glial fibrillary acidic protein and S-100B in hippocampus and cortex of diabetic rats: effects of vitamin E. Eur J Pharmacol 2003; 462: 67-71.
23. Bardoux P, Bichet DG, Martin H, et al. Vasopressin increases urinary albumin excretion in rats and humans: involvement of V2 receptors and the renin-angiotensin system. Nephrol Dial Transplant 2003; 18: 497-506.
24. Bardoux P, Bruneval P, Heudes D, Bouby N, Bankir L. Diabetes-induced albuminuria: role of antidiuretic hormone as revealed by chronic V2 receptor antagonism in rats. Nephrol Dial Transplant 2003; 18: 1755-63.
25. Bankir L, Roussel R, Bouby N. Protein- and diabetes-induced glomerular hyperfiltration: role of glucagon, vasopressin, and urea. Am J Physiol Renal Physiol 2015; 309: F2-23.
26. Bolignano D, Zoccali C. Vasopressin beyond water: implications for renal diseases. Curr Opin Nephrol Hypertens 2010; 19: 499-504.
27. Tonneijck L, Muskiet MH, Smits MM, et al. Glomerular hyperfiltration in diabetes: mechanisms, clinical significance, and treatment. J Am Soc Nephrol 2017; 28: 1023-39.
28. Imamura T, Kinugawa K, Hatano M, et al. Low cardiac output stimulates vasopressin release in patients with stage d heart failure. Circ J 2014; 78: 2259-67.
29. Niizuma S, Iwanaga Y. Revisiting vasopressin and heart failure. Expert Rev Cardiovasc Ther 2013; 11: 1451-4.
30. Bardoux P, Bankir L. Vasopressin contributes to hyperfiltration, albuminuria, and renal hypertrophy in diabetes mellitus: study in vasopressin-deficient brattleboro rats. Proc Natl Acad Sci 1999; 96: 10397-402.
31. Bardoux P, Bichet DG, Martin H, et al. Vasopressin increases urinary albumin excretion in rats and humans: involvement of V2 receptors and the renin-angiotensin system. Nephrol Dial Transplant 2003b; 18: 497-506.
32. Vinod P, Krishnappa V, Chauvin AM, Khare A, Raina R. Cardiorenal syndrome: role of arginine vasopressin and vaptans in heart failure. Cardiol Res 2017; 8: 87-95.
33. Jungen C, Scherschel K, Eickholt C, Kuklik P. Disruption of cardiac cholinergic neurons enhances susceptibility to ventricular arrhythmias. Nat Commun 2017; 8: 14155.